Am J Transl Res 2021;13(1):88-101
www.ajtr.org /ISSN:1943-8141/AJTR0111972

Original Article

Diffusion-weighted imaging with background body signal suppression (DWIBS) distinguishes benign lesions from malignant pulmonary solitary lesions

Chunli Zhao[1*], Dong Deng[2*], Wei Ye[2*], Liling Long[2], Yumin Lu[1], Youyong Wei[1]

[1]*Department of Radiology, People's Hospital of Guangxi Zhuang Autonomous Region, Nanning, China;* [2]*Department of Radiology, The First Affiliated Hospital of Guangxi Medical University, Nanning, China.* [*]*Equal contributors.*

Received April 5, 2020; Accepted July 18, 2020; Epub January 15, 2021; Published January 30, 2021

Abstract: This study aimed to determine applicable value of DWIBS in diagnosis of solitary pulmonary lesions. This study involved 32 solitary lung disease patients. T1W1, T2W1, T2WI-SPAIR were examined using MRI scanner and analyzed with View-forum 6.0 workstation. Imaging characteristics of pulmonary solitary lesions on DWIBS and ADC when b=300, 500 and 800 s/mm^2 were observed. Signal-to-noise ratio (SNR), contrast-noise-ratio (CNR) and ADC value of lesions under different b-values were measured. Image quality in different b-values was compared by analyzing SNR and CNR. ADC values of benign and malignant lesions in different b-value groups were tested using *t*-test. ROC curve was used to evaluate diagnostic efficacy of ADC value, and obtain diagnostic threshold. The results indicated that SNR and CNR value of 300 and 500 s/mm^2 group was significantly higher compared to 800 s/mm^2 group (P<0.05). When b-value was assigned as 500 s/mm^2, DWIBS demonstrated better and ideal images. ADC value of malignant lesions in different b-values was significantly lower compared to benign lesions (P<0.05), suggesting ADC value is a feasible approach for distinguishing benign from malignant lesions. AUC value of b=500 s/mm^2 was significantly higher compared to b=300 and b=800 s/mm^2 group (P<0.05). When b-value was assigned as 500 s/mm^2, the best ADC threshold value was 1.435×10^{-3} mm^2/s, with high sensitivity, specificity and accuracy of 80.0%, 83.3% and 84.4%, respectively. In conclusion, quantitative analysis of DWIBS examination and ADC value was helpful for qualitative diagnosis of pulmonary solitary lesions, and demonstrated potential to distinguish benign and malignant pulmonary solitary lesions.

Keywords: Solitary pulmonary lesions, magnetic resonance imaging, diffusion-weighted imaging with background body signal suppression, apparent diffusion coefficient

Introduction

Lung cancer is one of the most common malignant tumors clinically [1, 2]. According to the data provided by World Health Organization (WHO), the incidence and mortality of lung cancer are increasing significantly in the world [3]. In recent years, the incidence of lung cancer in China is also increasing year by year. In year of 2000, an investigation surveying lung cancer in China shows that the death rate of men is 40.1/100000, and that of women is 13.48/100000 [4]. Most of the lung cancer patients in clinical diagnosis has been the late stage, therefore, patients only administrate with the palliative treatment for prolonging survival. The early diagnosis and accurate staging of lung cancer determine the operation mode and treatment strategy, both of which are critical to improve survival rate and prognosis of patients.

Presently, computed tomography (CT), as a preferred examination method for lung lesions, plays an important role in quantitative and qualitative diagnosis, preoperative staging and post-treatment evaluation of lung tumors [5, 6]. However, CT also demonstrates a few shortcomings, including the low specificity of diagnosis and difficulty to understand the tumor blood supply and microcirculation. Nowadays, medical imaging has been developed from the

initial morphological examination to functional evaluation, and gradually from the macro-field to the micro-field. Take the molecular imaging for example, which can provide more detailed and objective imaging data for clinical practice, and can help clinical examination of diseases (especially tumors) earlier, so as to significantly improve the therapeutic effect [7]. As a non-radiation and non-invasive examination method, magnetic resonance imaging (MRI) is characterized by high contrast resolution, multi-parameter imaging, no-reconstruction of any cross-section imaging, no-bone artifacts and no-radiation damage [8]. At the same time, MRI can also reflect the histological characteristics of lesions to a certain extent through examining the signal intensity [5]. Therefore, MRI plays an increasingly important role in medical activities. However, the previous MRI usually results in the lower quality of lung imaging and lower signal-to-noise ratio (SNR). Moreover, MRI is only limited to the study of mediastinal lymph nodes, chest wall and pleural lesions, while the study investigating pulmonary parenchymal lesions is less. In recent years, with the rapid development of MRI software and hardware equipment and imaging technology, especially for the clinical application of 3.0T MRI scanner, the signal-to-noise ratio (SNR), resolution and scanning speed of MIR have been significantly improved [5,9]. All of the above backgrounds provide the wide prospect for application of MRI in lung parenchyma.

Diffusion weighted imaging (DWI) of MRI is a kind of functional imaging technology developed in recent years. Nowadays, DWI is the only non-invasive imaging method that can perform diffusion imaging and measurement of water molecules *in vivo* [10]. DWI, as an early diagnostic strategy, can detect the abnormal characteristics of lesions before the visual changes of conventional image morphology [11], measure the apparent diffusion coefficient (ADC) quantitatively [12], so as to make early differential diagnosis of lesions from metabolic function. Diffusion imaging plays an important role in displaying sensitivity and differential diagnosis of diseases, such as central nervous system [12, 13] However, due to the influence of respiration, heart beat and magnetic sensitive artifacts, application of lung DWI in diagnosis of lung tumors is still in the initial stage [14].

According to the limitations of traditional DWI imaging methods, Takahara et al. [12] developed a novel imaging method, named as "diffusion weighted imaging whole body imaging with background signal suppression (DWIBS)", to obtain thin-layer DWI. DWIBS can provide multi-level stimulation and signal average times in a slightly long time, can effectively inhibit fat by using short T1 inversion recovery (STIR)-EPI sequence, all of which improve the quality of 3D reconstruction image of whole body imaging [12]. DWIBS demonstrates a good background signal suppression, which can display the lesions and lymph nodes in a stereoscopic and intuitive way. Through the black-and-white reversal technology, DWIBS could achieve the similar effect with pet, and obtain PET-like image. DWIBS has been widely applied in the clinical diagnosis of brain, nerve and pelvic diseases [15-17]. The latest research [18] also shows that the lung DWIBS can obtain high quality DWI images. At present, many researches [19, 20] show that it is a hot topic to display lung diffusion images in lung tissues. It can be seen from the above results that imaging sequence and parameters are different due to the different MR scanning equipment. Therefore, the criteria for selecting the best b value of chest DWI is still uncertain, and ADC values vary greatly in different studies.

In this study, the Philips InteraArchieva 3.0T double gradient superconducting MRI scanner was used, and the b values of background signal suppression diffusion weighted imaging was set as b=300 s/mm^2, 500 s/mm^2 and 800 s/mm^2, respectively. Therefore, this study aimed to determine application value of background inhibition diffusion weighted imaging in diagnosis of solitary pulmonary lesions and optimize b value.

Materials and methods

Subjects

This study involved 32 patients diagnosed as solitary lung disease in Guangxi Medical University from March 2011 to March 2013. There were 20 males and 12 females, aging from 25 to 75 years, with an average age of

50.88±15.63 years. The diameter of lesions ranged from 1.4 to 10.0 cm, with an average diameter of 4.72±2.67 cm.

This study has been approved by Ethical Committee of People's Hospital of Guangxi Zhuang Autonomous Region, Nanning, China. All of the involved patients have provided the written formed consents and approved this study.

Inclusion criteria of patients

In this study, the patients complied with the following items have been involved in this study: ① The CT images show solitary solid nodule or mass in the lung tissues. ② The patients can cooperate with MR scanning. ③ The patients have not been administrated with any anti-tumor treatment before MR scanning. ④ There is no contraindication of MRI in subjects. ⑤ The data of patients with solitary pulmonary lesions were confirmed by the pathology or clinical follow-up.

MRI preparation

Before MRI examination, the inspection physician should describe the examination process to the subjects and obtain their cooperation, finally eliminating the tension of subjects. Keep the patients in a stable state of mind, so as to avoid the movement of the body caused by sudden discomfort. The subjects should take the supine position and hold the head with both hands. The respiratory gating sensor was tied to the most obvious part of the abdomen or chest which fluctuated with the breath movement. The front coil was covered on the chest and the back coil was placed on the back, the front coil and the back coil were aligned, and the front coil was fixed with the abdominal belt. The abdominal belt was tighten as much as possible without affecting the subject's breathing, and the subjects should be informed keep breathing evenly as much as possible to reduce the respiratory motion artifacts.

In this study, the T1W1, T2W1, T2WI-SPAIR were examined using Philips Intera Archieva 3.0T double gradient superconducting MRI scanner (Philips, Holland, Switzerland) and the corresponding software. Meanwhile, the SENSE-XL-TORSO body phased array surface coil was applied.

Routine MRI examination

Prior to DWIBS examination, all patients were administrated with the T1WI, T2WI, T2WI-SPAIR scans. T1WI: The turboflashecho (TEF) scanning was conducted with the a series of parameters, including TR/TE=10/2.3 ms, layer thickness of 7 mm, spacing of 1 mm, excitation (NSA) 1 of one time, field of vision (FOV) with 360 mm, matrix of 256×256 and scanning time of 100 s. T2WI: The single shot turboflashecho (SSTSE) scanning was conducted with the following parameters: TR/TE=2300/85 ms, breath trigger at the end of breath, layer thickness of 7 mm, layer spacing of 1 mm, excitations (NSA) of 1 time, FOV of 360 mm, matrix of 256×256 and scanning time of 72 s. T2WI weighted the fat suppression: The sense single-shot spectrum turbospin/spectrally selective attenuated inversion recovery (SSHH/SPAIR) was conducted with the following parameters, including TR/TE=1240/84, layer thickness of 7 mm, layer spacing of 1 mm, excitation (NSA) of one time, FOV of 360 mm, matrix of 256×256 and scanning time of 2-3 min.

DWIBS scan

Sensitivity encoding (SENSE) and single shot sensitivity-echo-planar imaging (SE-EPI) sequence were conducted for triggering the fat suppression. In this study, the DWIBS was conducted using b=300 s/mm^2, 500 s/mm^2 and 800 s/mm^2, respectively. For above three b values, the other parameters were same as the followings: 80 mT/m for high gradient mode, sense acceleration factor of 2, TR of 7000 ms, TE of 56 ms, layer thickness of 4 mm, layer spacing of 1 mm. Diffusion sensitive gradient was applied before and after 180° pulse, and different intensity of diffusion sensitive gradient was used for imaging. The other parameters were listed as the followings: NSA of 2, TI of 235 ms, EPI factor of 39, acquisition for 150 layers, matrix of 256×256, acquisition time for 5-7 min. MPR and 3D MIP reconstruction images were displayed using the black and white flipping technology.

MRI image analysis and measurement of index

At the end of the MRI scan, a series of MRI image information was transmitted to the View forum 6.0 workstation (Philips, Holland,

Switzerland). All the analyses were observed and analyzed by two radiologists who were engaged in chest imaging diagnosis under condition of unknown pathological results.

Measurement of ADC value of lesions under different b values: ADC data measurement was directly carried out on ADC diagram using the View forum 6.0 workstation (Philips, Holland, Switzerland). Referring to the conventional T2WI and T1WI images, the maximum diameter of lesion was selected on ADC curve. Region of interest (ROI) with the same size was selected from different locations of each focus, and View forum 6.0 workstation was placed in solid part of focus with uniform signals. During the measurement, the lesion edge and visible necrosis area should be avoided, taking the average value (mm^2/s as ADC value unit) for 3 times. When setting the position of different ROIs, all of which in different b-value images of each patient should be consistent as much as possible. For different b values, the region of interest should be taken at the same location on the same level.

Single noise ratio (SNR): The calculation formula for SNR was listed as follow: $SNR=S_{disease}/SD_{noise}$. In the formula, "$S_{disease}$" was the signal intensity of lesion, and SD_{noise} was the standard deviation for signal intensity of background noise at corresponding level. Both of them can be directly measured on DWIBS image. The measurement method for $S_{disease}$ was equal to that of ADC value. Then, ROI of the same area and quantity was placed at the external air background of the same layer (frequency coding direction) [12, 21].

Contrast noise ratio (CNR): CNR was calculated as follow: $(S_{disease}-S_{muscle})/SD_{noise}$, among which the $S_{disease}$ was the signal intensity of lesion, S_{muscle} was the signal intensity of lesion in the same layer of chest wall muscle, and SD_{noise} was the standard deviation of background noise signal intensity of corresponding layer. The measurement of $S_{disease}$ and SD_{noise} was the same as signal-to-noise ratio, and then ROI of the same amount and area was placed in the chest wall muscle of the same level. Eventually, the average value was obtained to obtain the final measurement data.

Moreover, the imaging characteristics for the pulmonary solitary lesions on DWI and ADC images were also observed for b=300 s/mm^2, b=500 s/mm^2 and b=800 s/mm^2, respectively.

ADC diagnostic criteria

The normal test was conducted for ADC value. Meanwhile, the Student's *t* test was also conducted for analyzing ADC values between benign lesion group and malignant lesion group. ROC curve method was used to evaluate the diagnostic efficiency of ADC value in order to obtain the diagnostic threshold of ADC value. If the ADC value was lower than the threshold value, it was defined as the malignant, while if it was higher than the threshold value, it was defined as benign.

Statistical analysis

In this study, SPSS 13.0 software (SPSS, Inc., Chicago, IL, USA) was used for statistical analysis of data. The CNR and SNR data between different b-value groups were analyzed using one-way ANOVA. The ADC values of benign and malignant lesions in different b value groups were analyzed using Student' *t* test. The *p* value less than 0.05 was assigned as significant difference.

The sensitivity, specificity and accuracy of different thresholds were also calculated. The receiver operating characteristic (ROC) curve under each b-value condition were drawn, and the areas under curve (AUC) of which were compared. Meanwhile, the identifying efficacy of ADC value on solitary benign and malignant lesions in different b-value groups was also evaluated. AUC was considered to significant when the value ranging from 0.5 to 1.0. The larger the AUC was, the higher the diagnostic efficiency was. Moreover, the ADC value with high sensitivity, specificity and accuracy under the optimal b-value condition was defined as the diagnostic threshold value.

Results

Basic data for patients

There were 33 lesions in 32 patients, among which there were 17 malignant tumors (18 lesions), including 13 lung cancers (13 lesions in 5 adenocarcinoma, 3 squamous cell carcinoma, 3 bronchioloalveolar carcinoma, 1 large

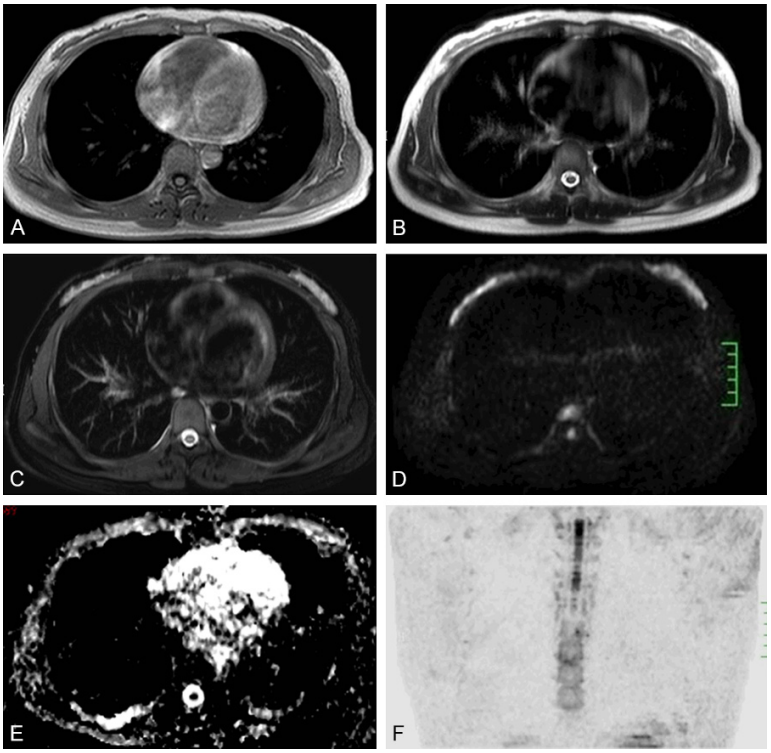

Figure 1. Manifestation for the normal chest MRI, DWIBS and ADC images. A. T1WI image. B. T2WI image. C. T2WI-SPAIR image. D. DWIBS image. E. ADC image. F. MPR image.

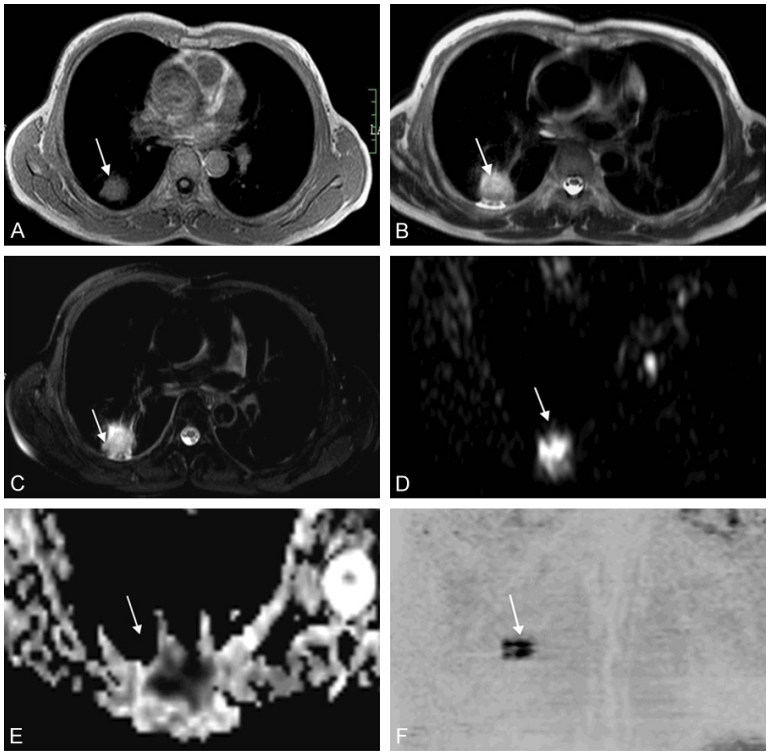

Figure 2. A patient, female, 65 years old. One month ago, nodular shadow was found in the dorsal segment of the lower lobe of the right lung (white arrow, b=500 s/mm^2). A. Transverse T1WI showed a isointensity signal of lesion. B and C. Transverse T2WI and T2-SPAIR images showed a hyper-intensity lesion with hazy border. D. Transverse DWIBS image showed a hyper-intensity lesion, which centre was more obvious. E. The corresponding level ADC image showed a hypo-intensity lesion, which centre was more obvious. The ADC value of the lesion was 0.56×10^{-3} mm^2/s. F. Making MPR reconstruction and black-white flip to get imitation PET effect. It showed a focal increased signal intensity area in lung field.

cell carcinoma, 1 sarcomatoid carcinoma), 1 malignant lymphoma (1 lesion), 1 malignant solitary fibroma (1 lesion), 2 lung metastases (3 lesions). Meanwhile, there were 15 cases of patients with 15 benign lesions, including 6 tuberculoma, 3 inflammations, 2 inflammatory pseudotumors, 2 hamartoma, 1 benign solitary fibroma and 1 pulmonary abscess.

Normal chest MRI, DWIBS and ADC manifestation

For the chest wall muscles, the signal intensity of T1WI (**Figure 1A**) and T2WI (**Figure 1B**) was moderate, that of T2 was slightly low (**Figure 1C**), and that of DWIBS (**Figure 1D**) and ADC (**Figure 1E**) was equal.

There was a low signal on T1WI, T2WI, T2WI, DWIBS and ADC in the cortex of ribs, sternum and thoracic vertebrae (**Figure 1**). Because bone marrow is rich in fat, it showed slightly hyper-intensity signal on T1WI and T2WI, slightly low signal on T2WI, and low signal on DWIBS and ADC (**Figure 1**). Because there were many hematopoietic cells in the bone marrow of

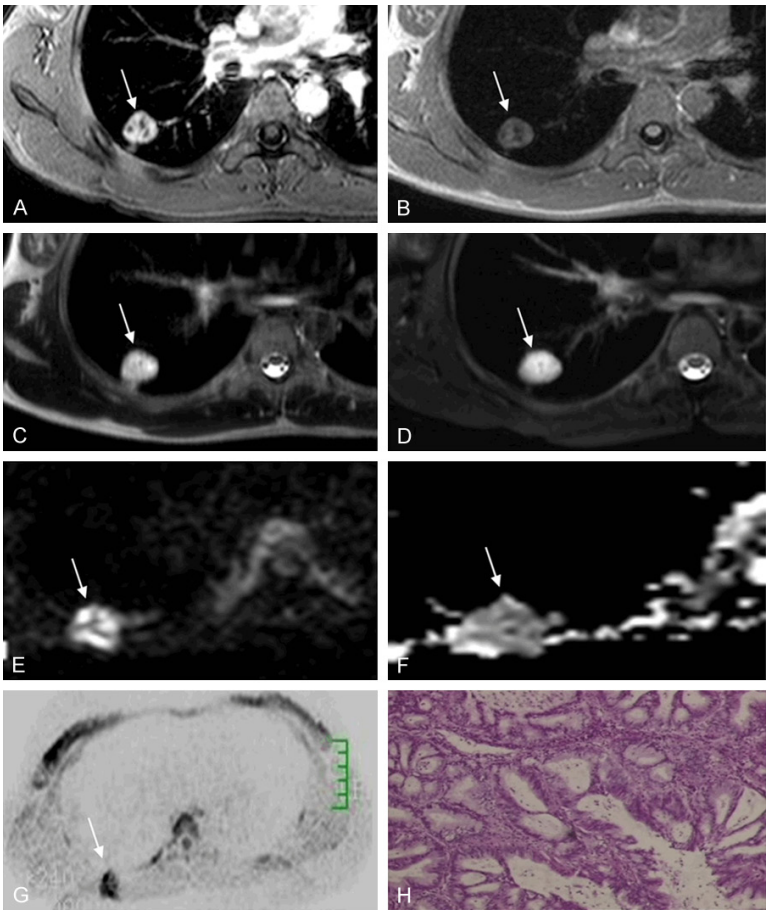

Figure 3. A patient, Female, 33 years old, illustrating the nodular shadow of the dorsal segment of the lower lobe of the right lung tissue (b=500 s/mm^2). A. MRI enhancement scan showed a non-homegeneous enhancement lesion with a non-enhancement liquefied necrotic area. B. Transverse T1WI showed a uneven isointensity lesion. C and D. Transverse T2WI and T2-SPAIR image showed a hyper-intensity lesion. E. Transverse DWIBS image showed a hyper-intensity lesion, with a small patchy hypo-intensity. F. The corresponding level ADC image showed a hypo-intensity lesion, which ADC value was 0.98×10^{-3} mm^2/s. G. Imitation PET showed a focal increased signal intensity area in lung field. H. HE staining of biopsy (magnification, 200×) showed a right lower lobe mucinous adenocarcinoma accompanied by necrosis.

thoracic vertebrae, the signal was hyper on DWIBS and low on ADC (**Figure 1**). Pulmonary parenchyma, tracheobronchial, cardiac chamber and large vessels were all illustrated as black on T1WI, T2WI and T2WI, and low signal on DWIBS and ADC (**Figure 1**).

MRI, DWIBS and ADC manifestation of solitary pulmonary lesion

Manifestation of peripheral lung cancer (13 lesions in 13 cases*) (**Figures 2, 3**):* Among 13 lesions, 10 were round-like and 3 were irregular. T1WI of 13 lesions showed slightly low or isointensity signal. For the T2WI, there were obvious hyper-intensity signals in 2 lesions, slightly hyper-intensity signals or isointensity signals in 10 lesions and slightly low signals in 1 lesion. For the T2-SPAIR, 10 lesions demonstrated as obvious hyper-intensity signals, and 3 lesions showed slightly hyper-intensity signals or isointensity signals. Moreover, 11 lesions demonstrated hyper-intensity signals on DWIBS and low signal on ADC, 2 lesions showed low signal on DWIBS and hyper-intensity signal on ADC.

Manifestation of Malignant solitary fibroma (1 lesion in 1 case) and malignant lymphoma (1 lesion in 1 case): For the malignant solitary fibroma, the lesion was round and the edge was clear. The signal was uneven, with isointensity signal on T1WI, slightly hyper-intensity signal on T2WI and T2-SPAIR, hyper-intensity signal on DWIBS, and low signal on ADC. For the malignant lymphoma, which had irregular shape and uneven signal. T1WI demonstrated isointensity signals, T2WI and T2-SPAIR with slightly hyper-intensity signals, DWIBS with hyper-intensity signal and ADC with low signal.

Manifestation of Metastasis (3 lesions in 2 cases): The lesions were round like, with smooth margin. The signals of two lesions were uniform, isointensity signals on T1WI, slightly hyper-intensity signals on T2WI and T2-SPAIR. For another 1 lesion, the signal was not uniform, with isointensity signals on T1WI, and higher signals on T2WI and T2-SPAIR. Three lesions showed slightly hyper-intensity signals on DWIBS and slightly low signal on ADC.

Manifestation of tuberculosis (6 lesions in 6 cases): Three lesions were round like and another 3 lesions were irregular. Six lesions

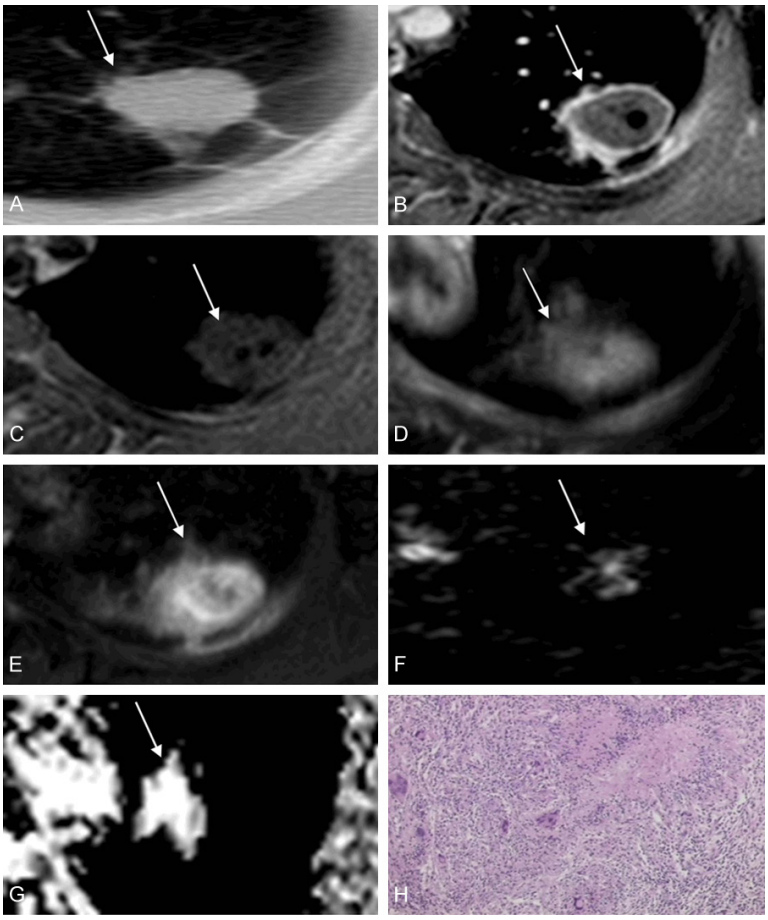

Figure 4. A patient, male, 30 years old, with symptom of dry-cough more than a month (b=500 s/mm^2). A. CT enhancement scan showed a mid-homogeneous enhancement lesion. B. MRI enhancement scan showed the significantly thin-walled ring enhancement of lesion. C. Transverse T1WI showed a uneven isointensity lesion. D and E. Transverse T2WI and T2-SPAIR image showed an uneven hypo-intensity lesion, which border was hazy. F. Transverse DWIBS image showed a hypo-intensity lesion. G. The corresponding level ADC image showed a hypo-intensity lesion, ADC value of which was 2.5×10^{-3} mm^2/s. H. HE staining of biopsy (magnification, 200×) showed a left upper lobe tuberculosis accompanied by caseous necrosis.

showed slightly low or isointensity signals on T1WI, one showed significantly hyper-intensity signals on T2WI, and five showed slightly hyper-intensity signals. T2-SPAIR showed slightly hyper-intensity signals in 1 lesion, and obvious hyper-intensity signals in 5 lesions. Four lesions showed low signal on DWIBS, hyper-intensity signal on ADC, while two lesions showed hyper-intensity signal on DWIBS, low signal on ADC (**Figure 4**).

Manifestation of hamartoma (2 lesions in 2 cases): The lesions were round like, with smooth edge and uniform signal. One lesion showed isointensity signal on T1WI, one showed slightly low signal. Two lesions showed hyper-intensity signals on T2WI and T2-SPAIR. Two lesions showed low signals in DWIBS and hyper-intensity signal in ADC (**Figure 5**).

Manifestation of inflammatory lesions (6 lesions in 6 cases): Two lesions were round like and four lesions were irregular. Five lesions showed slightly low or isointensity signals on T1WI, one showed slightly hyper-intensity signals. Three lesions showed hyper-intensity signal on T2WI, and three lesions showed slightly hyper-intensity signals. Six lesions demonstrated hyper-intensity signals on T2-SPAIR and two lesions showed low signal on DWIBS and higher signals on ADC. Two lesions illustrated hyper-intensity signal on DWIBS and low signal on ADC (**Figure 6**).

Manifestation of benign solitary fibroma (1 lesion in case): The lesion was round and the signal was even. The lesion showed isointensity signals on T1WI, slight hyper-intensity signals on T2WI, hyper-intensity signals on T2-SPAIR, low signals on DWIBS and hyper-intensity signals on ADC.

Comparison for SNR of DWIBS in different b-value groups

In all 32 patients of this study, there were 33 solitary pulmonary lesions. The SNR and CNR values measured with DWIBS images with different b-value diffusion sensitive gradient fields were listed in **Table 1**.

The ANOVA results showed that there were statistically significant differences for the SNR value among different b-value groups (**Table 1**, *P*=0.000). According to the LSD analysis, there was no significant difference for the SNR value between b=300 s/mm^2 group and b=500 s/

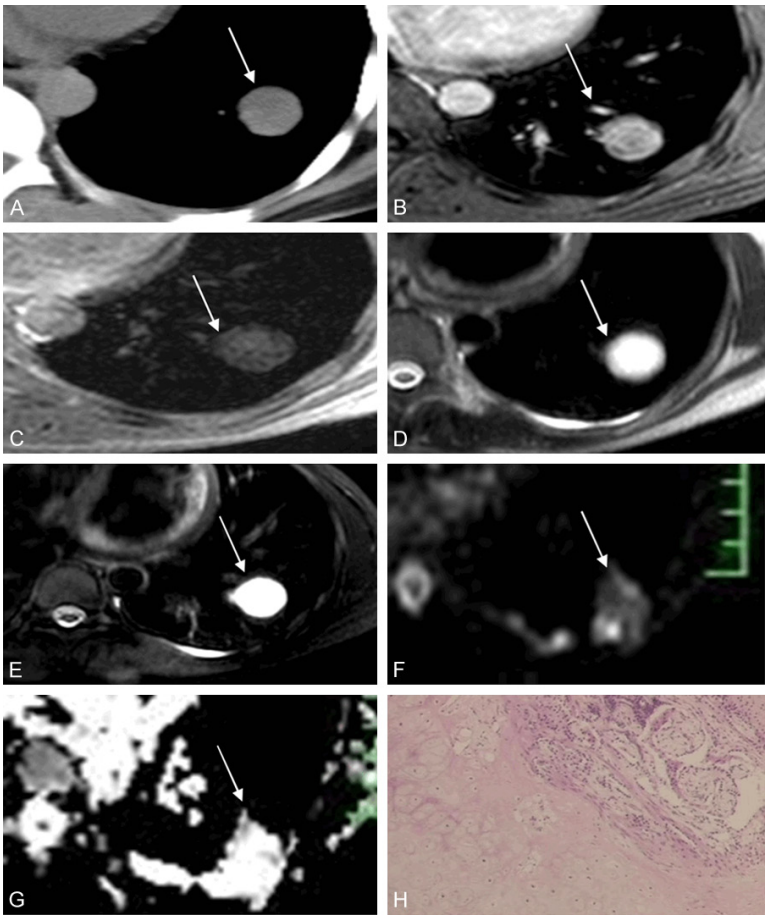

Figure 5. A patient, female, 34 years old, with symptom of cough more than a month, undergoing anti-inflective reexamine (b=500 s/mm^2). A. CT plain scan showed a round soft tissue density left lower lobe lesion with smooth border. B. MRI enhancement scan showed an uneven non-homegeneous enhancement lesion. C. Transverse T1WI showed an uneven isointensity lesion. D and E. Transverse T2WI and T2-SPAIR image showed a obvious hypo-intensity lesion. F. Transverse DWIBS image showed an uneven hypo-intensity lesion. G. The corresponding level ADC image showed a obvious hypo-intensity lesion, the ADC value of which was 3.5×10^{-3} mm^2/s. H. HE staining of biopsy (magnification, 200×) showed a left lower lobe hamartomatumors.

mm^2 group (**Table 1**, *P*>0.05). The SNR value of 300 s/mm^2 and 500 s/mm^2 group was significantly higher compared to that of 800 s/mm^2 group (**Table 1**, *P*<0.05). Moreover, with the increased b-values, the SNR value decreased, and the image quality also reduced (**Table 1**; **Figure 7**).

Comparison for CNR of DWIBS in different b-value groups

Based on ANOVA findings, there were significant differences for the CNR among different b-value groups (**Table 1**, *P*=0.000), among which b=500 s/mm^2 group illustrating larger CNR value. The LSD analysis indicated there were no significant differences for the CNR values between b=300 s/mm^2 group and b=500 s/mm^2 (**Table 1**, *P*>0.05). The CNR value in b=300 s/mm^2 group and b=500 s/mm^2 was significantly higher compared to that in b=300 s/mm^2 group (**Table 1**, *P*<0.05). According to data of **Figure 7** and **Table 1**, when the b-value was assigned as 500 s/mm^2, the MRDWIBS image demonstrated the higher SNR and CNR value, represented the ideal quality. Additionally, with the increased b-value, the CNR was firstly increased and then decreased.

Comparison for ADC values of benign and malignant solitary lesions with different b values

In this study, the patients were divided into benign lesions group (15 lesions in 15 cases) and malignant lesions group (18 lesions in 17 cases). The results indicated that ADC value of malignant lesions in different b-values (b=300 s/mm^2, b=500 s/mm^2 and b=800 s/mm^2) was significantly lower compared to that of benign lesions (**Table 2**, *t*=-3.250, -4.670, -2.554, respectively and *P*=0.003, 0.000, 0.016, respectively). These results suggest that ADC value is a feasible approach for distinguishing the benign lesions from malignant lesions.

ROC curve analysis

ROC curve was used to analyze ADC value of each b-value group for evaluating diagnostic efficacy of pulmonary benign and malignant lesions. The ROC curve showed that ADC values in three b-value groups demonstrated diagnostic significance (area under ROC curve >0.5). The area under ROC curve with b-value

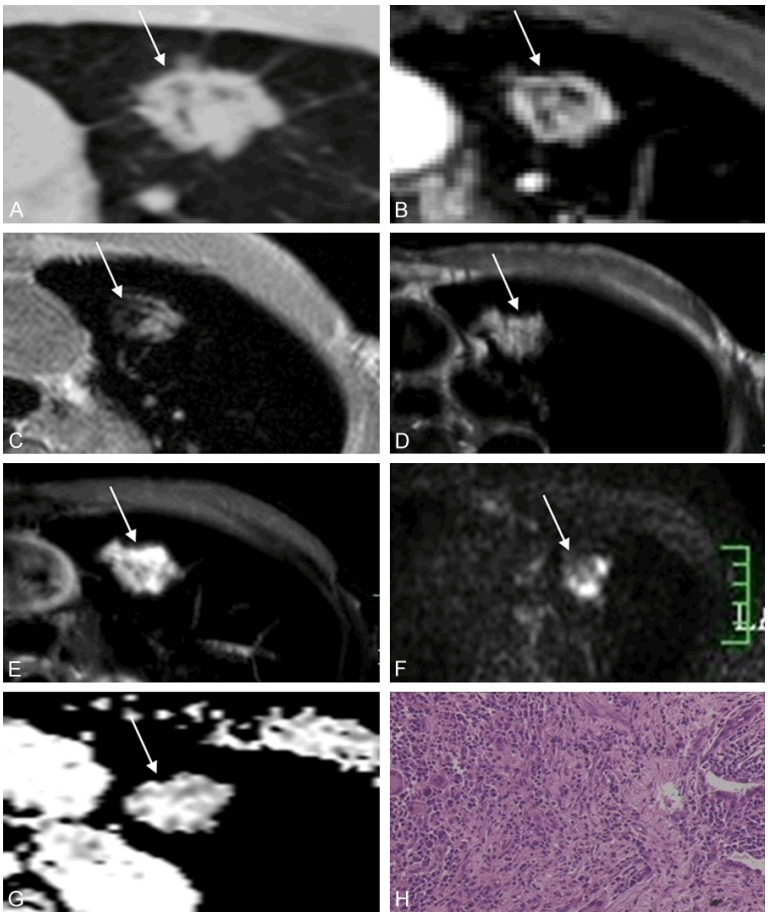

Figure 6. A patient, female, 72 years old, with a left-upper lobe lesion (b=500 s/mm^2). A. CT plain scan showed a irregular long shape lesion with hazy border. B. MRI enhancement scan showed a obvious enhancement lesion. C. Transverse T1WI showed an uneven isointensity lesion. D and E. Transverse T2WI and T2-SPAIR image showed an obvious hypo-intensity lesion. F. Transverse DWIBS image showed an uneven hypo-intensity lesion. G. The corresponding level ADC image showed an obvious hypo-intensity lesion, the ADC value of which was 2.1×10^{-3} mm^2/s. H. HE staining of biopsy (magnification, 200×) showed a left upper lobe inflammatory pseudotumors.

Table 1. Comparison for the SNR and CNR under three b values on DWIBS (mean ± SD)

b Values (s/mm^2)	No. of lesions (n)	Signal-noise ratio (SNR)	Contrast-noise ratio (CNR)
300	33	46.238±2.28	40.232±1.86
500	33	45.301±2.47	41.559±2.21
800	33	31.43±3.24	20.774±2.45
F Value		38.662	7.863
p Value		0.000	0.000

of 500 s/mm^2 was 83.0%, with the highest differential diagnosis efficiency (**Figure 8**; **Table 3**). The AUC value of b-value for 300 s/mm^2 and b-value for 800 s/mm^2 was 78.3% and 73.5%, respectively. According to the ROC curve, the best ADC threshold value for differential diagnosis of benign and malignant lesions, and the sensitivity, specificity and accuracy under this value were illustrated in **Table 3**. Therefore, when the b-value was assigned as 500 s/mm^2, the best ADC threshold value was 1.435×10^{-3} mm^2/s, with high sensitivity, specificity and accuracy of 80.0%, 83.3% and 84.4%, respectively (**Table 3**).

Discussion

Due to the limitation of breath holding time, the traditional DWI inevitably depletes part of image resolution and SNR. In view of the above limitation, Takahara et al. [12] developed a new imaging background signal suppression DWIB). DWIBS can display the lesions in the same way as positron emission tomography, directly and stereoscopically. Meanwhile, DWIBS can illustrate DWI with high resolution and measure ADC quantitatively. Because of the improved ADC image quality and accurate ADC value measurement, DWIBS has been widely applied in lung diseases [18, 22].

DWIBS is rarely used in evaluating pulmonary benign and malignant nodules or masses. Komori et al. [23] studied the value of DWIBS compared with PET in differentiating benign and malignant nodules or masses in lung, and proved that DWIBS was more specific than PET. Therefore, DWIBS is more valuable than PET in differentiating benign and malignant pulmonary nodules or masses. In recent years, DWIBS has been gradually applied

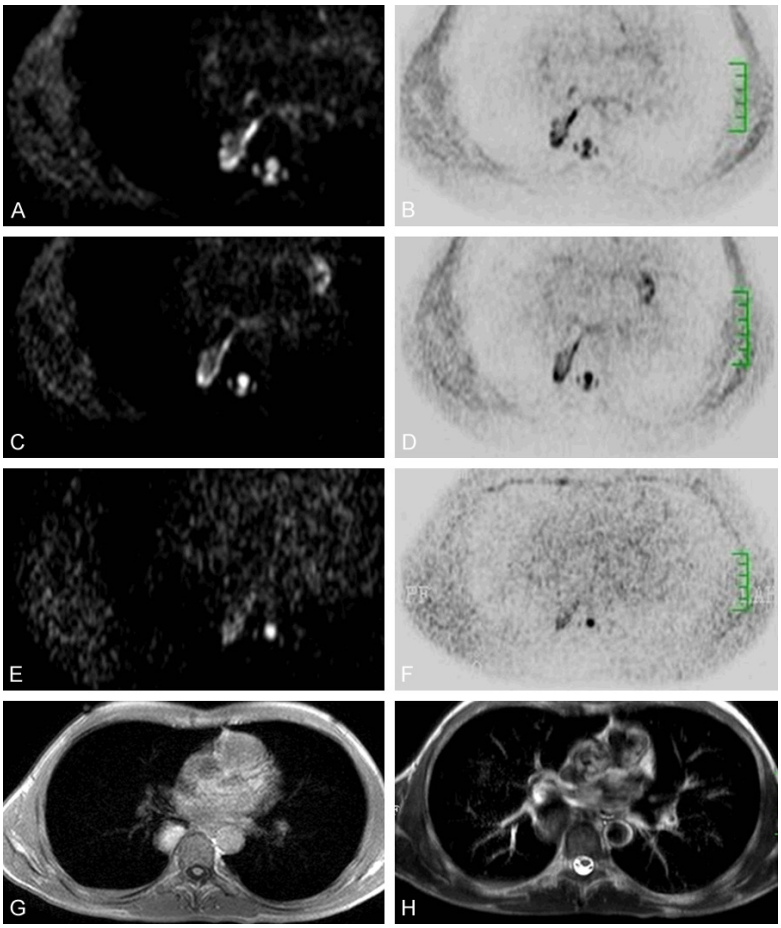

Figure 7. The DWIBS, imitation PET, T1WI and T2WI images for the pulmonary lesions under different b-values. A-F. The DWIBS, imitation PET images under 300, 500, 800 s/mm^2 showed that the SNR was decreased with the increase of b-value. There were no significant differences for SNR between b-value=300 s/mm^2 and 500 s/mm^2 and lesions were displayed clearly. The SNR obviously decline when the b-value was assigned as 800 s/mm^2, and the lesions were displyed fuzzily. G and H. Right lower lobe lesion was slightly hypo-intensity on the T1WI, and was isointensity on the T2WI.

Table 2. Comparison of ADC value (×10^{-3} mm^2/s) between solitary pulmonary malignant and benign lesions under three b values

Groups	No. of lesions (n)	b Values (s/mm^2)		
		300	500	800
Benign lesions	15	2.175±0.266	1.659±0.282	1.311±0.3
Malignant lesions	18	1.895±0.227	1.300±0.180	1.044±0.387
t Value		-3.250	-4.464	-2.554
p Value		0.003	0.000	0.016

in clinic, reflecting the information of pulmonary nodules or masses non-invasively. Therefore, DWIBS has also been opened up a new way for the differential diagnosis of benign and malignant pulmonary nodules or masses.

b-value, as a diffusion sensitive factor, can be selected by the operator in DWIBS inspection [24]. The selection of b-value can affect the DWIBS image quality, ADC value and accuracy [25], therefore, b-value selection is considered to be a very important parameter. The previous studies [26, 27] reported that the b-value mainly ranges from 0 s/mm^2 to 1000 s/mm^2 for the study of DWI and ADC values of lung tumors. Colagrande et al. [28] reported that the larger the b-value is, the worse the image quality is. When the b-value is more than 1000 s/mm^2, the SNR and spatial resolutions are lower, the magnetic sensitive artifacts are more serious, and the image quality is significantly reduced. Presently, DWI technology for qualitative analysis of pulmonary nodules or masses is the most recommended b-value (500-800 s/mm^2). Therefore, the numerical consistency is good. This study was conducted under the 3.0T high-field MRI equipment by selecting b-value of 300 s/mm^2, 500 s/mm^2 and 800 s/mm^2. The findings showed that SNR was higher when b value was assigned as 300 s/mm^2 and 500 s/mm^2. While, following with the increase of b-value, the SNR and image quality was decreased. According to the ANOVA results, there was significant difference for the CNR among different b-value groups (P=0.000), among which b=500 s/mm^2 group demonstrated the largest CNR. When the b-value was defined as 500 s/mm^2, DWIBS image demonstrated the higher SNR and CNR, and the better DWI image quality. Therefore, the b-value can be used for

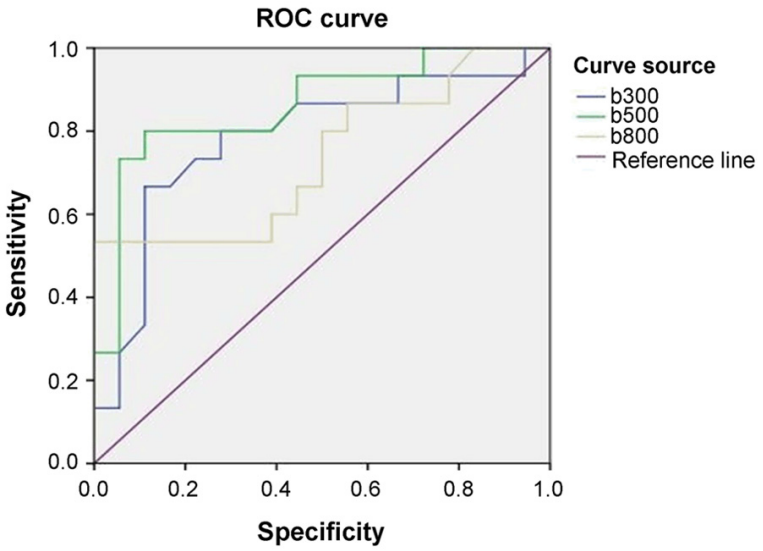

Figure 8. Three b-values ROC curve on ADC values.

ADC value measurement. Moreover, in this study, there was also significant difference for the ADC value between benign lesions and malignant lesions.

DWI is the an imaging method that can detect the micro-movement of water molecules in living tissues. Most of the benign lesions showed relatively complete cell structure in histology, with low cell proliferation, low cell density and large extracellular space [29]. Therefore, DWIBS signal is low and ADC value is increased. The lung parenchyma is very sensitive because of the lack of gas signal. Generally, most benign lesions show relatively low signal on DWIBS and high signal on ADC, while most malignant tumors show obvious high signal on DWIBS, low signal on ADC, low signal on necrotic cystic part, and high signal on ADC [11]. According to the above criteria, it has a certain value for the differential diagnosis of typical benign lesions and common malignant. Agnello et al. [30] found that 87% of benign lesions, such as focal nodular hyperplasia or adenoma in the liver, showed high signals on DWI. In this study, according to the above-mentioned typical benign lesions and common malignant tumors for DWIBS visual inspection criteria, the diagnostic coincidence rate was 80%. In this study, 20% patients didn't conform to the above two manifestations. Among which, 4 cases were benign lesions (2 tuberculosis, 2 inflammatory nodules), showing high signals on DWIBS and low signals on ADC, and 2 cases were malignant lesions (all peripheral lung cancer), showing low signals on DWIBS and high signals on ADC. The signals of benign and malignant lesions still overlapped to some extent and were not completely characteristic. Therefore, it is difficult to distinguish the nature of lesions only by signal characteristics, and it is necessary to use ADC value to analyze the lesions quantitatively.

It has been reported that DWI signal and ADC value of pulmonary solitary lesions play a certain role in differentiating benign from malignant. However, DWIBS is rarely used in the evaluation of pulmonary benign and malignant nodules or masses [18]. A previous study [31] showed that the ADC value of most malignant tumors was lower than that of benign tumors. However, due to the complexity and diversity of tumor cell components and internal structures of different pathological types, and the different levels of blood perfusion, there is a large degree of overlap between ADC values. Our study showed that b=500 s/mm^2 was the best b value for DWIBS in lung solitary benign and malignant lesions. Under this b-value, ADC values of benign and malignant lesions were (1.659±0.282)×10^{-3} mm^2/s and (1.300±0.180)×10^{-3} mm^2/s, respectively. The ADC value of malignant lesions was significantly lower compared to that of benign lesions. The results of this study are also consistent with the findings of the DWIBS focusing on the other parts [32, 33]. The previous studies [32, 33] reported that that there are high signals for the malignant lesions on DWIBS, and the ADC value of malignant lesions is significantly lower than that of benign lesions. Therefore, we believe that the quantitative analysis of ADC value is useful for the identification of pulmonary solitary lesions.

In this study, the ROC curve was drawn and the b-values of 300 s/mm^2, 500 s/mm^2 and 800 s/mm^2, were selected. respectively. The ADC value demonstrated the most effective

Table 3. The analysis results of three b-value ROC curve on ADC values

b Values (s/mm^2)	Area under curve (AUC)	ADC threshold (×10^{-3} mm^2/s)	Sensitivity (%)	Specificity (%)	Accuracy (%)
300	0.783	1.920	80.0	72.2	69.7
500	0.830	1.435	80.0	83.3	84.4
800	0.735	1.195	53.3	61.1	57.6

differential diagnosis for the pulmonary solitary benign and malignant lesions when the b-value was assigned as 500 s/mm^2. Under the b value of 500 s/mm^2, ADC value of 1.435×100^{-3} mm^2/s was taken as the diagnostic threshold value for the diagnosis of pulmonary solitary benign and malignant lesions, with the higher sensitivity, specificity and accuracy of 80.0%, 83.3% and 84.4% respectively. The present results showed that the ADC value measured by DWIBS demonstrated the potential to differentiate benign and malignant lung lesions. Moreover, DWIBS is also hopeful to become a new and useful tool for differential diagnosis. With the development of software and hardware technology of 3.0T or above ultra-high field strength equipment, the best value range for b-value in chest DWIBS and the threshold standard of ADC value to distinguish benign and malignant lesions need further study and confirmation in following studies.

There are still a few shortcomings in this study. Firstly, the whole time for scanning on 3.0 TMRI is relatively long, and the effect of respiratory and cardiac pulsation artifacts on the location and quality of lesions is large, all of which need to be analyzed in combination with conventional MRI images. Secondarily, DWIBS imaging showed that there was a large overlap between benign and malignant lesions. Thirdly, DWIBS suppresses the background signals and the image lacks enough anatomical information. Fourthly, for some small lesions (less than 1.0 cm in the lung), DWIBS demonstrated poor display ability.

In conclusion, this study attempted to explore the application value of DWIBS in diagnosis of 32 cases of pulmonary solitary benign and malignant lesions and optimize the best b-value and improved the quality of DWI images using 3.0T MRI DWIBS. Our results showed that when b-value was assigned as 300, 500 and 800 s/mm^2, the SNR and CNR of image decreased with the increase of b-value. The SNR and CNR values of b=300 s/mm^2 and b=500 s/mm^2 group were significantly higher compared to that of b=800 s/mm^2. The ADC value of malignant lesions was significantly lower compared to that of benign lesions. When b-value was assigned as 500 s/mm^2, the area under ROC curve was the largest, indicating that the b-value demonstrates the highest diagnostic efficiency. The sensitivity, specificity and accuracy for the DWIBS was 80%, 83.3% and 84.4%, respectively. Therefore, the quantitative analysis of ADC value is helpful for the qualitative diagnosis of pulmonary solitary lesions, and demonstrates the potential to distinguish benign and malignant pulmonary solitary lesions.

Disclosure of conflict of interest

None.

Address correspondence to: Dr. Chunli Zhao, Department of Radiology, People's Hospital of Guangxi Zhuang Autonomous Region, 6 Taoyuan Road, Nanning 530001, China. Tel: +86-0771-2186543; Fax: +86-0771-2186543; E-mail: zlc-5281990@163.com

References

[1] Han B, Wu J and Huang L. Induction of apoptosis in lung cancer cells by viburnum grandiflorum via mitochondrial pathway. Med Sci Monit 2020; 26: e920265.

[2] Zhao D, Liu H, Liu H, Zhang X, Zhang M, Kolluri VK, Feng X, He Z, Wang M, Zhu T, Yan X and Zhou Y. Downregulated expression of hsa-circ-0037515 and hsa-circ-0037516 as novel biomarkers for non-small cell lung cancer. Am J Transl Res 2020; 12: 162-170.

[3] Borczuk AC. Prognostic considerations of the new World Health Organization classification of lung adenocarcinoma. Eur Respir Rev 2016; 25: 364-371.

[4] Yang RS. Epidemiology and new technologies for early detection of lung cancer. Chin J Cancer Prev Treat 2004; 11: 745-748.

[5] Chin AY, Jeon TY, Lee KS, Lee JH, Seo JB, Kim YK and Chung MJ. 3-T MRI: usefulness for evaluating primary lung cancer and small nodules in lobes not containing primary tumors. AJR Am J Roentgenol 2007; 189: 386-392.
[6] Huang C, Liang J, Lei X, Xu X, Xiao Z and Luo L. Diagnostic performance of perfusion computed tomography for differentiating lung cancer from benign lesions: a meta-analysis. Med Sci Monit 2019; 25: 3485-3494.
[7] Chen ZY, Wang YX, Lin Y, Zhang JS, Yang F, Zhou QL and Liao YY. Advance of molecular imaging technology and targeted imaging agent in imaging and therapy. Biomed Res Int 2014; 2014: 819324.
[8] Lee JY, Kang BS, Shim HS, Song IH, Kim M, Lee SH, Chung HW, Lee MH and Shin MJ. Clear cell hidradenoma: characteristic imaging features on ultrasonography, computed tomography and magnetic resonance imaging. J Ultrasound Med 2018; 37: 1993-2001.
[9] Bammer R. Basic principles of diffusion-weighted imaging. Eur J Radiol 2003; 45: 169-184.
[10] Chen X, Jiang J, Shen N, Zhao L, Zhang J, Qin Y, Zhang S, Li L and Zhu W. Stretched-exponential model diffusion-weighted imaging as a potential imaging marker in preoperative grading and assessment of proliferative activity of gliomas. Am J Transl Res 2018; 10: 2659-2668.
[11] Koh DM and Collins DJ. Diffusion-weighted MRI in the body: applications and challenges in oncology. Am J Roentgenol 2007; 188: 1622-1635.
[12] Takahara T, Imai Y, Yamashita T, Yasuda S, Nasu S and Van Cauteren M. Diffusion weighted whole body imaging with background body signal suppression (DWIBS): technical improvement using free breathing, STIR and high resolution 3D display. Radiat Med 2004; 22: 275-282.
[13] Restrepo L, Jacobs MA, Barker PB and Wityk RJ. Assessment of transient ischemic attack with diffusion-and perfusion-weighted imaging. AJNR Am J Neuroradiol 2004; 25: 1645-1652.
[14] Matoba M, Tonami H, Kondou T, Yokota H, Higashi K, Toga H and Sakuma T. Lung carcinoma: diffusion-weighted mri imaging-preliminary evaluation with apparent diffusion coefficient. Radiology 2007; 243: 570-577.
[15] Sun M, Cheng J, Zhang Y, Bai J, Wang F, Meng Y and Li Z. Application of DWIBS in malignant lymphoma: correlation between ADC values and Ki-67 index. Eur Radiol 2018; 28: 1701-1708.
[16] Balaji R, Devi R and Stumpf J. Diffusion-weighted whole-body imaging with background body signal suppression (DWIBS-application in planning for cyberknife therapy in patients with gliomas. Pract Radiat Oncol 2013; 3: S35.
[17] Mürtz P, Krautmacher C, Traber F, Gieseke J, Schild HH and Willinek WA. Diffusion-weighted whole body MR imaging with background body signal suppression: a feasibility study at 3.0 tesla. Eur Radiol 2007; 17: 3031-3037.
[18] Xu L, Tian J, Liu Y and Li C. Accuracy of diffusion-weighted (DW) MRI with background signal suppression (MR-DWIBS) in diagnosis of mediastinal lymph node metastasis of nonsmall-cell lung cancer (NSCLC). J Magn Reson Imaging 2014; 40: 200-205.
[19] Matoba M, Tonami H, Kondou T, Yokota H, Higashi K, Toga H and Sakuma T. Lung carcinoma: diffusion-weighted MRI imaging-preliminary evaluation with apparent diffusion coefficient. Radiology 2007; 243: 570-577.
[20] Satoh S, Kitazume Y, Ohdama S, Kimula Y, Taura S and Endo Y. Can malignant and benign pulmonary nodules be differentiated with diffusion-weighted MRI? Am J Roentgenol 2008; 191: 464-470.
[21] Uto T, Takehara Y, Nakamura Y, Naito T, Hashimoto D, Inui N, Suda T, Nakamura H and Chida K. Higher sensitivity and specificity for diffusion-weighted imaging of malignant lung lesions without apparent diffusion coefficient quantification. Radiology 2009; 252: 247-254.
[22] Sommer G, Wiese M, Winter L, Lenz C, Klarhofer M, Forrer F, Lardinois D and Bremerich J. Preoperative staging of non-small cell lung cancer: comparison of whole-body diffusion-weighted magnetic resonance imaging and 18F-fluorodeoxyglucose-positron emission tomography/computed tomography. Eur Radiol 2012; 22: 2859-2867.
[23] Komori T, Narabayashi I, Matsumura K, Matsuki M, Akagi H, Ogura Y, Aga F and Adachi I. 2-[Fluorine-18]-fluoro-2-deoxy-D-glucose positron emission tomography/computed tomogrpahy versus whole-body diffusion-weighted MRI for detection of malignant lesions: initial experience. Ann Nucl Med 2007; 21: 209-215.
[24] Zhang L, Xiao T, Yu Q, Li Y, Shen F and Li W. Clinical value and diagnostic accuracy of 3.0 T multi-parameter magnetic resonance imaging in traumatic brachial plexus injury. Med Sci Monit 2018; 2: 7199-7205.
[25] Cova M, Squillaci E, Stacul E, Manenti G, Gava S, Simonetti G and Pozzi-Mucelli R. Diffusion-weighted MRI in the evaluation of renal lesions: preliminary results. Br J Radiol 2004; 77: 851-857.
[26] Nakayama J, Miyasaka K, Omatsu T, Onodera Y, Terase S, Matsuno Y, Cho Y, Hida Y, Kaga K and Shirato H. Metastases in mediastinal and hilar lymph nodes in patients with non-small cell lung cancer: quantitative assessment with

diffusion-weighted magnetic resonance imaging and apparent diffusion coefficient. J Comput Assist Tumogr 2010; 34: 1-8.
[27] Kanauchi N, Oizumi H, Honma T, Kato H, Endo M, Suzuki J, Fukaya K and Sadahiro M. Role of diffusion-weighted magnetic resonance imaging for predicting of tumor invasiveness for clinical stage IA non-small cell lung cancer. Eur J Cardiothorac Surg 2009; 35: 706-711.
[28] Colagrande S, Carbone SF, Carusi LM, Cova M and Villari N. Magnetic resonance diffusion-weighted imaging: extra neurological applications. Radiol Med 2006; 111: 392-419.
[29] Kusunoki T, Murata K, Nishida S, Tomura T and Inoue M. Histopathological findings of human thyroid tumors and dynamic MRI. Auris Nasus Larynx 2002; 29: 357-360.
[30] Agnello F, Ronot M, Valla DC, Sinkus R, Van Beers BE and Vilgrain V. High-b-value diffusion-weighted MR imaging of benign hepatocellular lesions: quantitative and qualitative analysis. Radiology 2012; 262: 511-519.
[31] Wang YX, Yuan MZ and Wen ZX. Application of apparent diffusion coefficient and exponent apparent diffusion coefficient values in magnetic resonance imaging diffusion-weighted imaging to differentiate benign and malignant ovarian epithelial tumors. J Cancer Res Ther 2016; 12: 401-405.
[32] Tamai K, Koyama T, Saga T, Umeoka S, Mikami Y, Fujii S and Togashi K. Diffusion-weighted MR imaging of uterine endometrial cancer. J Magn Reson Imaging 2007; 26: 682-687.
[33] Akduman EI, Momtahen AJ, Balci NC, Mahajann N, Havlioglu N and Wolverson MK. Comparison between malignant and benign abdominal lymph nodes on diffusion-weighted imaging. Acad Radiol 2008; 15: 641-646.